

# A Brief Introduction to Linear Optical Quantum Computing

By Ruchi Pendse

<b>Abstract</b>	<b>2</b>
<b>Introduction</b>	<b>2</b>
<b>DiVincenzo's criteria for quantum computation</b>	<b>2</b>
<b>Basics of Linear Optical Quantum Computing</b>	<b>3</b>
Types of Photonic Qubits	3
Sources of Photons	4
Gate operations	4
Single Qubit Gates	4
Rotation Gates	4
Knill-Laflamme-Milburn Protocol	5
C-Z Implementation	5
Experimental Implementation of the CNOT Gate	6
Cluster State Computation	7
<b>Gates in Trapped Ion and Superconducting Systems</b>	<b>7</b>
<b>Building an Ion-Photon Quantum Network</b>	<b>8</b>
Ion-Photon Interaction in Trapped-Ion systems	8
<b>Sources of noise and errors</b>	<b>9</b>
Noise in Photonic Systems	9
Noise in Trapped Ion systems	9
Noise in Superconducting Systems	10
<b>Scaling</b>	<b>10</b>
<b>Conclusion</b>	<b>10</b>

# Abstract

Linear optical quantum computing is one of the systems used to implement quantum computation. The use of linear optical components in generation, detection and manipulation of photons in single and two-qubit operations is described. The Knill-Laflamme-Milburn theorem on the scalability of the linear optical system is explained, as is the relatively new cluster state method of computation.

Superconducting and trapped ion architectures are briefly described, and a comparison is made with respect to ability to implement gates and scalability.

# Introduction

Over the years, many systems have been proposed to realize quantum computation. Some examples include superconductors, trapped ions, nitrogen vacancy centers, and photonic systems. Trapped ion quantum computation utilizes ions confined in radio frequency traps as qubits. Ions of an element are all identical, and the energy levels within an ion can be used to encode a two-level system, making them an intuitive choice for qubits.

Much like trapped ions, photons also make for an obvious choice for a quantum computing system. They are found in nature, are decoherence-free, and their vertical and horizontal polarizations can encode a two-level system, making a single qubit. Moreover, a photonic system can be easily integrated to the existing classical communication architecture, which can be utilized for quantum communication.

Superconducting systems introduce anharmonicity in a superconducting circuit by using a Josephson junction. The anharmonic levels of the subsequent harmonic oscillator are used as the qubit levels.

# DiVincenzo's criteria for quantum computation

In the year 2000, DiVincenzo laid out five key conditions for a system to be able to implement quantum computation, and two additional conditions that would be required to implement a quantum network. The conditions are as follows (DiVincenzo, 2000):

1. That the system must be scalable and have well-characterized qubits
2. The qubits must be capable of being initialized
3. Decoherence times must be longer than the gate operation times
4. A universal set of gates must be implementable
5. The system must have qubit specific measurement capability
6. There must be a way to convert stationary qubits to flying qubits for communication
7. The flying qubits must be faithfully transmitted to a specified location

A photonic system of computation meets five of the seven aforementioned conditions, but fails in assembling a universal gate set, due to the difficulty in achieving photon-photon interaction, and in faithful transmission of flying qubits, which relies on high-fidelity optical quantum memories.

On the other hand, trapped ions and superconducting systems meet all the key conditions with high fidelity of operation.

## Basics of Linear Optical Quantum Computing

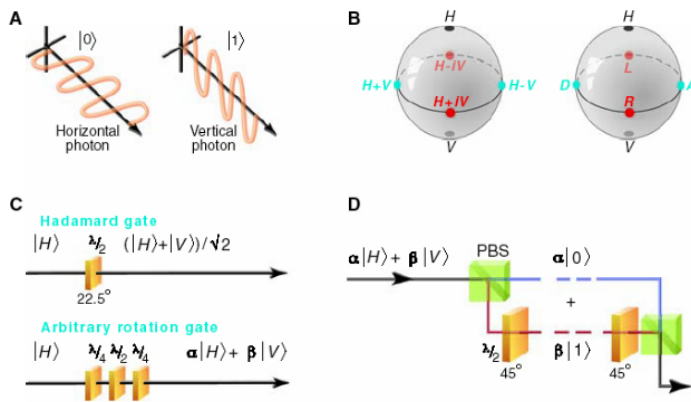


Fig. 1. (A) In linear optical systems, horizontal polarization represents a logical ‘0’ and vertical polarization represents a logical ‘1’; (B) The Bloch sphere representation of the qubits. D and A are diagonal and antidiagonal states, where  $|D\rangle = |1\rangle + |0\rangle$  and  $|A\rangle = |1\rangle - |0\rangle$ . Right circular state  $|R\rangle$  is represented as  $|0\rangle + i|1\rangle$  and left circular state  $|L\rangle$  as  $|0\rangle - i|1\rangle$ .

(C) Birefringent plates are used to carry out single qubit operations, which work by retarding one polarization by some wavelength  $\lambda$  relative to a polarization orthogonal to it, which causes a rotation of the state on the Bloch sphere. The axis of rotation is determined by the Bloch sphere. A Hadamard gate can be realized by a  $\lambda/2$  waveplate oriented at  $22.5^\circ$ .

(D) A polarizing beam splitter converts between polarization and path encoding. A  $\lambda/2$  waveplate oriented at  $45^\circ$  transforms vertical states to horizontal states and vice-versa.

## Types of Photonic Qubits

Since photons do not naturally interact, direct entangling schemes are difficult to implement. Thus, a probabilistic approach to entanglement is utilized, in which the spatial modes of the photon store the information. This is known as **dual-rail encoding**. The orthogonal polarizations of the photon (vertical and horizontal, for example), are the most common pairs of modes, but other degrees of freedom, such as transverse, spatial, frequency, and temporal-bin modes have also been used for dual-rail encoding. (Kok et al., 2007)

Dual-rail encoding can represent a qubit with two spatial modes. Here, the qubit of choice is a single photon of two modes:

$$|0\rangle_L = |1\rangle \otimes |0\rangle \equiv |1, 0\rangle, \quad |1\rangle_L = |0\rangle \otimes |1\rangle \equiv |0, 1\rangle.$$

Single-rail encoding is also possible for photonic qubits, which rely on using only one mode of the photon per qubit. Thus, the qubit is given by the vacuum and a single-photon state. However, deterministic two-qubit operations require the addition of non-linearities (such as Kerr nonlinearities) while using single-rail encoded qubits.

Time-bin qubits make use of the late/early arrival of photons at the detectors, and are encoded using the arrival paths. However, they are not commonly implemented in linear optical systems because of the additional detector-dependence which they require.

Single qubit operations are implemented using beam splitters and phase shifters, which correspond to  $\sigma_x$ ,  $\sigma_y$ , and  $\sigma_z$  rotations.

## Sources of Photons

There are two mainly used schemes of single-photon sources:

1. Spontaneous Parametric Down Conversion (SPDC)
2. cavity-QED Raman schemes

While SPDC produces single photons of Gaussian distribution, the latter scheme produces photons of Lorentzian wave packets. In 2005, Rohde, Ralph and Nielsen (Rohde et al., 2005) proved that sources generating Gaussian wave packets are more robust than those creating Lorentzian wavepackets, which is why SPDC is more commonly used to generate single photons.

Spontaneous Parametric Down Conversion works by using a short-wavelength pump laser to generate photon pairs of longer wavelength by passing the beam through a birefringent crystal. To maintain high state quality, the pump power is kept low, which increases the amount of time it takes to generate sufficient single photons.

Other photon sources such as quantum dots, which may yield photons on demand at a higher rate of generation, cannot be used due to spectral differences between the dots, which will lead to distinguishable generated photons.

## Gate operations

### Single Qubit Gates

#### Rotation Gates

All single qubit gates can be performed using beam splitters and phase shifters. Phase shifters introduce a phase to the incoming photons, whereas beam splitters split the incident beam of light into two beams, which can be used in generating an interference. A polarizing beam splitter is used to split the incident beam according to the polarization of the photons. Mirrors completely reflect the incident light, and are used to direct the incoming photons to the other optical components.

The unitaries for these components are as follows (Knill et al., 2001):

$$U(\mathbf{B}_{\theta,\phi}) = \begin{bmatrix} \cos \theta & -e^{i\phi} \sin \theta \\ e^{-i\phi} \sin \theta & \cos \theta \end{bmatrix},$$

Here,  $\theta$  and phase angle  $\phi$  depend on the reflection and transmission amplitudes of the media.

$$R(\theta) = \begin{bmatrix} \cos \theta & -\sin \theta \\ \sin \theta & \cos \theta \end{bmatrix}.$$

Since the reflecting rate of a mirror is 1, it implements a rotation gate.

$$U(\mathbf{P}_\phi) = \begin{bmatrix} e^{i\phi} & 0 \\ 0 & 1 \end{bmatrix} = \begin{bmatrix} e^{i\phi/2} & 0 \\ 0 & e^{-i\phi/2} \end{bmatrix}$$

The Knill-Laflamme-Milburn protocol found that optical quantum computing can be carried out solely by linear optical components. They employed the NS gate and the aforementioned linear optical components to implement CNOT logic. (Knill et al., 2001)

## Knill-Laflamme-Milburn Protocol

The Knill-Laflamme-Milburn protocol lays out the method to implement two-qubit interactions using only linear optical components, in which a CZ gate is implemented using a nonlinear sign shift gate.

The Hong-Ou-Mandel effect describes two-photon interference, in which two photons are simultaneously made incident on a 50:50 beam splitter. Depending upon their overlap, the photons may exit the beam splitter simultaneously and get detected. Highly distinguishable photons are more likely to enter two different beam splitters, and not interfere. The observation of an interference pattern using an interferometer confirms the indistinguishability of the photons, thus proving their interaction.

This effect is used in facilitating photon interactions to create two-qubit gates.

The KLM scheme also utilizes a nonlinear sign gate. The core concept of the KLM protocol relies on postselection, in which operations are carried out only if two interacting photons are detected together. If the system experiences photon loss, the operations in the rest of the pipeline are not carried out.

Knill, Laflamme and Milburn proposed that such postselected measurements would introduce nonlinearities in the system, and use two ancilla photons for measurement.

The nonlinear sign-shift (NS) gate is often used to carry out operations in linear optical quantum computing. It is made using beamsplitters to which identical beams of single mode photons are shone.

## C-Z Implementation

The gate uses two NS gates which change the relative phase of the two input qubits. The simultaneous detection of both photons is ensured due to the Hong-Ou-Mandel effect. The two photons enter the first beam splitter of the NS gate, and recombine after the second beam splitter, where a phase of  $\pi$  is introduced if both incoming photons were in the  $|1\rangle$  state.

As the success probability of each NS gate used in this operation is  $\frac{1}{4}$ , the probability of the CZ gate successfully working is  $\frac{1}{16}$ . This is slower than a classical computer if  $n$  CZ gates were to be successively performed.

As linear optical quantum computing makes use of heralded states of the system, a failure in the operations destroys the qubits.

To overcome the low probability of success, and to make the operation deterministic instead of probabilistic, the KLM protocol makes use of quantum teleportation.

In the teleportation trick proposed by Gottesman and Chuang, the information in the two qubits which are to be acted upon by the CZ gate are first teleported from one mode to a different mode. This preserves the information in case of qubit destruction/photon loss.

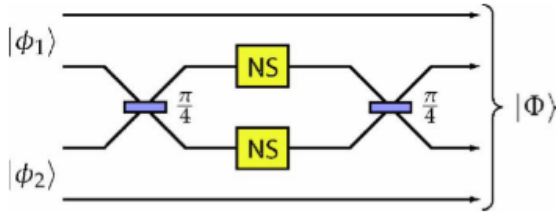


Fig 2. Implementation of the CZ gate using two NS gates (Kok et al., 2007)

### Experimental Implementation of the CNOT Gate

There have been many experimental implementations of probabilistic CNOT gates. In 2003, Pittman et al. implemented a 3-photon CNOT gate in which the control and ancilla are generated using SPDC and the target is generated by an attenuated laser pulse. The set up consists of these three qubits, as well as two polarizing beam splitters.

The control and target qubits are initially in an arbitrary, two-qubit state, while the ancilla is prepared in a superposition of horizontal and vertical polarization.

The three qubits are passed through a polarizing beam splitter, which transforms them to:

$$|\psi\rangle_{\text{out}} \propto |H\rangle_a U_C |\psi\rangle_{\text{in}} + |V\rangle_a \tilde{U}_C |\psi\rangle_{\text{in}} + \sqrt{6} |\xi\rangle_{\text{act}},$$

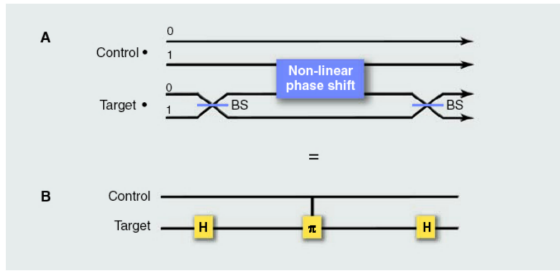
In this state, the  $U_c$  is the CNOT operator between the control and target modes, and the state  $\xi$  represents  $n$  photons in modes  $a$ ,  $c$ , or  $t$  (ancilla, control, or target).

The ancilla qubit is then measured, and the transform is applied to the target and control qubits. If the ancilla measurement yields a vertical polarization ( $V_a$ ), the target undergoes a bit flip, and the CNOT operation is performed.

The experimental error in this gate is 21%, with a success probability of  $\frac{1}{4}$ .

To make near-deterministic CNOT gates, a single logical qubit is encoded into several physical qubits. Thus, information will be preserved regardless of qubit loss errors. However, implementing near-deterministic entangling gates has a large overhead of preparing and storing several qubits at once.

To mitigate this problem, a non-deterministic solution using cluster states was proposed in 2001.



(O'brien, 2007)

Fig. 3. (a) Schematic representation of a possible CNOT gate using NS gates. (b) The working of a Hadamard gate is done using beam splitters.

## Cluster State Computation

Cluster state computation or one-way quantum computation makes use of teleportation to reduce the overheads incurred in entangling operations in linear optical computing. Cluster state computation is based on the projective measurement model, and not the circuit model of quantum computation.

Here, the quantum information encoded in a set of qubits is teleported to a new set using entanglement and single-qubit measurements. This way, single-qubit measurements are only performed on the cluster one column of qubits at a time, and this outcome determines the basis in which the succeeding column will be measured. (Raussendorf et al., 2009)

## Gates in Trapped Ion and Superconducting Systems

In a superconducting system, single qubit gates are achieved using microwave pulses which are sent to the transmission line coupled with the qubit. The frequency of the controlling pulse is the resonant frequency that allows transitions between the energy levels of the qubits. This way, depending on the duration of the applied pulse, rotations along the Bloch sphere can be implemented. (Krantz et al., 2019)

Two-qubit gate implementations require the qubits to be coupled together. This can be achieved using capacitive or inductive coupling, in which both qubits are connected to the respective active element, and the pulse driving the operation causes changes in the capacitance or inductance, thus changing the current directed to the qubits.

In trapped ion systems, methods to carry out single qubit rotations differ depending on the type of qubit. For hyperfine qubits, single qubit gates are implemented using Raman transitions or microwave pulses which drive the rotation. Transitions can be achieved in optical qubits with single resonant pulses, and Zeeman qubits can be manipulated using a radio frequency drive. Cirac and Zoller first proposed an entangling gate operation, which uses the shared motional modes of the ions as an information bus to transmit information between them. The CZ (Cirac-Zoller) gate is a C Phase gate, which can be transformed to a CNOT gate using single qubit rotations. (Bruzewicz et al., 2019)

A drawback of the CZ gate was the need to bring the motional modes back to the ground state. Molmer and Sorensen's implementation of the controlled phase gate eliminated this requirement, and thus MS gates have become the more commonly used gates in trapped ion systems today.

The fidelities for these gate operations are really high in trapped ion systems, with optical qubits having gate operations performed in the microsecond range, with fidelities as high as 99.995%.

## Building an Ion-Photon Quantum Network

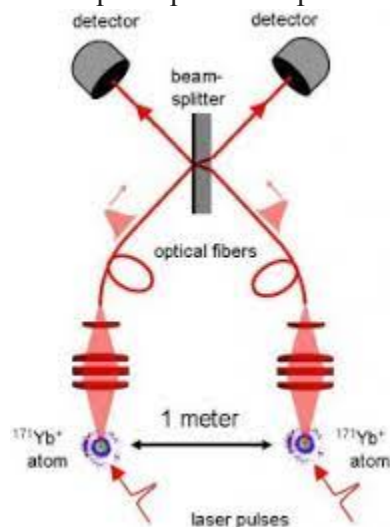
Robust quantum computation requires the presence of a quantum bus to help carry out operations on remote qubits, and a quantum memory to store and transport quantum information within a network. Photons are the obvious choice for flying qubits, due to their speed of transport, and pre-existing classical optical telecommunication network that can be utilized in quantum networks. (Monroe)

### Ion-Photon Interaction in Trapped-Ion systems

Most quantum computing hardware systems today use photonic interconnects to work as flying qubits, in order to make remote entanglement/interactions possible.

Trapped ion systems have long coherence times, but shuttling ions between sections in the system becomes difficult. Thus, ion-photon pairing is utilized, where a beam of light is shone to an ion, emitting a photon that it becomes entangled with. For remote entanglement, the photons emitted by the different ions are collected and directed to a 50:50 beam splitter that projects the entanglement onto the corresponding ions. A “double-click” is observed at the detectors, which heralds the entanglement of the two ions. (Blinov et al., 2004)

Multi-qubit quantum operations can then be carried out on the remotely entangled ions.



(Monroe)

Fig. 4. Entangling operation between remote  $\text{Yb}^+$  ions.



# Sources of noise and errors

## Noise in Photonic Systems

Implementation of quantum computation systems must be robust enough to sources of errors that the unavoidable defects in hardware do not result in erasure or decoherence of the quantum information.

In linear optical qubits, the sources of noise arise from material defects in the media that make up the birefringence plates, half and quarter wave plates, photon detectors, and beam splitters.

Moreover, circuit errors and low-fidelity quantum memories also add to loss of quantum information and additional errors.

Photon detectors can lead to two types of errors: 1) photon loss, where the detector counts too few photons, and 2) dark counts, where non-existent photons are counted by the detector.

The use of avalanche photodiodes as bucket photon detectors can also lead to photon loss, as the nanoseconds of dead time due to reversal of voltage does not allow for photon detection. (Kok et al., 2007)

Components such as beam splitters, half and quarter wave plates, and birefringent plates are made of dielectric media which might have a small absorption amplitude. This may lead to unwanted photon scattering, and thus qubit and information loss. Moreover, unwanted birefringence in the dielectric media will also lead to photon squeezing.

The use of nonidentical wavepackets in interferometric setups or mismatched impedances at boundaries of the dielectric material may lead to mode mismatching, which will interfere with consequent computation (for example, mismatched modes in photons will not allow the logically correct function of a CNOT or a CPhase gate).

Quantum memories are required to store photons while offline preparation of entangled states takes place. Fiber optic loops, while readily available due to existing classical infrastructure, induce a very high photon loss ( $0.17 \text{ dB km}^{-1}$  at  $1550 \text{ nm}$ ).

Noisy photon sources, especially deterministic sources such as photons derived from quantum dots, or ions, or vacancy centers in diamonds, can lead to simultaneous emission of multiple photons, and nonidentical photons (depending on their modes), which are useless for entanglement and computation.

Thus, error correction schemes in linear optical quantum computation are carried out for three main types of errors: 1) inefficient detectors, 2) noisy photon sources, and 3) unfaithful quantum memories.

## Noise in Trapped Ion systems

The trapped-ion system of computation also faces challenges with regards to photodetectors, and similar detector errors are observed. (Bruzewicz et al., 2019)

Moreover, depending on the type of qubit used in the system, errors may arise due to the effect of electromagnetic fields. The motional modes of the ions also contribute to motional heating, which can decohere states. This can be corrected using control pulses and sympathetic cooling,

but control sequences themselves can add to the errors due to crosstalk and unwanted ionic interactions.

The difficulty in scaling in both systems arises due to the bulky optical equipment (lasers for photon generation and cooling), and photodetectors and optical plates in linear optical systems. Addressability in trapped-ion systems becomes cumbersome with unfocused/incorrectly positioned beams driving ions neighbouring the ones that have been targeted.

## Noise in Superconducting Systems

Types of noise present in quantum systems can be categorized into systematic and stochastic noise. Systematic noise is caused by a control or readout error in a process. For example, an improperly tuned control pulse would bring an incorrect degree of rotation to the qubit upon which it is acting. Due to the nature of systematic errors, they can be corrected once identified. On the other hand, stochastic errors arise due to random fluctuations of parameters which can get coupled to the qubit. Fluctuating electromagnetic fields on the surface of the chip (metal surface/substrate surface) can couple to the qubit and create unknown or uncontrolled fluctuations in other qubit parameters and lead to decoherence.

As each superconducting chip used must be individually fabricated, the resulting fabrication errors also impart a degree of randomness to the functioning of the qubit.

## Scaling

Optical components like lasers, beam splitters, and other dielectric media to operate on generated photons make both trapped ion and linear optical systems bulky. Thus, both systems would benefit from integrated quantum photonics and electronics.

A crucial component in integrated photonics is the optical waveguide, which is an optical fiber fabricated into the chip substrate. Depending on the width and thickness of the fiber, the allowed spatial modes and polarization of photons that are transmitted can be controlled. Since both linear optical systems, and trapped ion systems using photonic interconnects require the use of single-spatial mode photons, the integrated optical fiber can be fabricated accordingly. (Slussarenko & Pryde, 2019)

In trapped ion systems, delivery of light can be done by coupling into waveguides along the chip's edge, or using grating couplers. This will also reduce the possibility of crosstalk.

The use of integrated optics can improve the collection efficiency of the detectors, and detector errors of photon loss can thus be reduced. Moreover, integrated optics would improve routing times for photons to shuttle within the system (in the case of photon-ion interconnects).

Integrated quantum photonics will be greatly beneficial in advancing quantum key distribution technologies. Due to the pre-existing optical fiber network used in classical telecommunications, an integrated photonic chip that generates, prepares and detects photons will make QKD simpler to execute.

## Conclusion

As of today, single qubit rotations can be performed with 99.9999% fidelity and two-qubit

entangling operations can be performed with 99.9% fidelity in trapped ion systems. Similarly, single qubit gate fidelity in superconducting systems is 99.92%, and 99.4% for two-qubit gates. Linear optical systems, on the other hand, have a very small probability of successful operations ( $\frac{1}{4}$  probability of success in Pittman's implementation of the CNOT gate).

Both trapped ions and linear optical qubits show long coherence times, but with the slow rate of generation of optical qubits, and the high error rates in fiber loop quantum memories used in linear optical systems, trapped ions and superconducting systems outshine linear optics in this metric as well.

Photonic qubits would allow for easy integration to pre-existing telecommunications architecture, but other systems using photonic interconnects can also easily tap into this resource for communication applications.

Overall, both trapped ion and superconducting systems satisfy the five core DiVincenzo criteria whereas linear optical qubits do not, and thus, the former two architectures are more capable to perform quantum computations today.

## References

- Blinov, B., Moehring, B., & Monroe, C. (2004). Observation of entanglement between a single trapped atom and a single photon. *Nature*, 428, 153-157.
- Brown, K., Chiaverini, R., & Sage, J. (2021). Materials challenges for trapped-ion quantum computers. *Nature Reviews Materials*.
- Bruzewicz, C., Chiaverini, J., & McConnel, R. (2019). Trapped-Ion Quantum Computing: Progress and Challenges. *Applied Physics Reviews*, 6(2).
- DiVincenzo, D. P. (2000). The physical implementation of quantum computation. *Fortschritte der Physik: Progress of Physics*, 48.
- Knill, E., Laflamme, R., & Milburn, G. J. (2001). A scheme for efficient quantum computation with linear optics. *Nature*, 409(6816), 46-52.
- Kok, P., Munro, W. J., & Nemoto, K. (2007). Linear optical quantum computing with photonic qubits. *Reviews of modern physics*, 79.

- Krantz, P., Kjaergaard, M., Yan, F., & Orlando, T. P. (2019). A quantum engineer's guide to superconducting qubits. *Applied Physics Reviews*, 6(2).
- Kriesch, A. (n.d.). *File:Paul-Trap.svg*. Wikimedia Commons. Retrieved November 23, 2021, from <https://commons.wikimedia.org/wiki/File:Paul-Trap.svg>
- Monroe, C. (n.d.). *Ion-Photon Quantum Networks – Trapped Ion Quantum Information*. Trapped Ion Quantum Information.  
<https://iontrap.umd.edu/research/ion-photon-quantum-networks/>
- O'brien, J. (2007). Optical quantum computing. *Science*, 318.
- Ralph, T. C., & Pryde, G. J. (2010). Optical quantum computation. *Progress in optics*, 54.
- Raussendorf, R., Browne, D. E., & Briegel, H. J. (2009). Measurement-based quantum computation with cluster states. *International Journal of Quantum information*, 7(6), 1-53-1203.
- Rohde, P., Ralph, P., & Nielsen, M. (2005). Optimal photons for quantum-information processing. *Physical Review A*, 72.
- Slussarenko, S., & Pryde, G. J. (2019). Photonic quantum information processing: A concise review. *Applied Physics Reviews*, 6.